Silicon (2024) 16:3491–3501
https://doi.org/10.1007/s12633-024-02932-x

RESEARCH

Effect of Temperature and Method of Synthesis on Morphology and Phase Transition of Amorphous and Crystalline Nano Silica Extracted from Mission Grass (Pennisetum Polystachion)

Ajmal Thayyullathil[1] · C. M Naseera[1] · F. M Liyakhath[1] · E. K Vydhehi[1] · S. R Sheeja[1] · Subair Naduparambath[1] · Swetha Sasidharan[2]

Received: 24 November 2023 / Accepted: 25 February 2024 / Published online: 9 March 2024

Abstract

Bio silica nanoparticles are well accepted candidates in the field of material science. The present study conveys that Mission grass (MG) is a potential source of bio silica and to best of our knowledge no studies have been reported so far in connection with the extraction of silica from MG. Herein, we have demonstrated the synthesis of nano silica from MG by acid leaching and sol gel method. The effect of annealing temperature of MG and method of synthesis on the morphology and phase transition were studied. Four forms of silica viz 600 °C Acid Leached Silica (600ALS), 600 °C Sol Gel Silica (600SGS), 850 °C Acid Leached Silica (850ALS), 850 °C Sol Gel Silica (850SGS) have been synthesized through acid leaching and sol gel process. The 600SGS possess an average size of 40–100 nm and are found to be in amorphous form, whereas 850 SGS is more agglomerated with size of more than 100 nm and is in crystalline form. A similar trend is also observed in the case of silica nanoparticles that were obtained from the acid leached process. The phase purity as well as the crystalline nature of the all samples are studied by using XRD, FT-IR, FESEM-EDS. Crystallinity Indices are calculated and was highest for 850SGS (82%) and the lowest for 600SGS (43%). From the EDS data, it was found that the percentage of silica was the highest (95.61%) for 600SGS and the lowest (91.95%) for 850ALS. The thermogravimetric studies revealed that the crystalline silica (850 SGS) is more hygroscopic than amorphous silica, but later has more internal water due to its porous nature. Hence, it can be utilized as an excellent moisture absorber.

Keywords Mission Grass · Acid Leached Silica · Sol Gel Silica · Crystallinity · Characterization

1 Introduction

Silicon is the second most abundant element by mass in the earth crust which primarily exist as silica (SiO_2) in different crystalline forms such as quartz, crystoballite, tridymite and amorphous forms such as silica gel, kieselguhr etc. Silica nanoparticle is one of the most accepted nanoparticles in the field of material science and in research field due to their facile synthesis, rich surface chemistry, low toxicity, easily tunable mechanical, optical, electrical properties, and their high thermal stability [1]. Silica nanoparticles have wide applications in the field of advanced catalysis [2], drug delivery [3], biomedical applications [4], polymer composites [5], concrete filler [6], anticorrosion agents [7] etc. Amorphous silica is extensively used in micro encapsulation [8], stabilizing agents in therapeutics [9] etc. Nano silica in crystalline form is also used in photovoltaic cell [10], ceramics [11], humidity sensors [12] etc. Silica nanoparticles are effective against COVID-19 also [13].

Statement of Novelty The paper presents a comprehensive study on the effect of calcination temperature and method of synthesis on morphology and other properties of crystalline and amorphous silica prepared from Mission Grass. MG is an aggressive and invasive weed, widely distributed in agricultural fields and other natural habitats of Kerala, India. It has no economic importance except it is used as fodder but most of the cattle are not fond of this as a food. To the best of our knowledge, no studies have been reported with respect to the extraction of nano silica from MG, although bio silica was extracted from other sources. In this work, nano silica is extracted in amorphous and crystalline form through acid leaching and sol gel process, thus making it as a value-added product. The structural features, morphology, crystallinity, and thermal behavior of different products are investigated and compared.

Extended author information available on the last page of the article

Nano silica is prepared by methods like vapour phase reduction, sol gel method, thermal reduction, acid leaching etc. Conventionally, nano silica is extracted from synthetic organic precursors like Tetraethyl orthosilicate [14] but this method is costly and not eco-friendly. In recent years agricultural products, agricultural wastes and other biomasses are considered as the best raw material for making value added products. Plants especially those under the class of grass family take up silica during their growth and when they are burned, organic components will decompose, and the remaining ash contains silica as the major products [15]. Many natural sources are also used to prepare nano silica [16]. The most used raw material is rice husk [17]. Numerous studies were conducted on bio silica synthesized from rice husk. Nano silica is also prepared from rice straw [18], lemon grass [19], corn cob [20], sugarcane bagasse [21], banana stem [22], elephant grass [23] etc.

Mission grass (Pennisetum Polystachion) is an aggressive, invasive, perennial grass widely distributed in India, tropical Africa, Australia etc. and they compete with native species, disturb crops, and expand rapidly. They spread through agricultural and natural habitats and along the roadsides [24]. Thus, it is considered a weed in most countries. Due to heavy monsoon, which covers half of the year, the expansion of MG in Kerala (One of the states in India) is very rapid and it creates ecological problem. Not only a big threat to the agricultural crops but also it facilitates frequent fire at the fields and forests. No specific use is reported for MG except as fodder. Some studies were reported regarding the production of ethanol from MG [25]. Nevertheless, it is assumed that MG is a rich source of bio silica and no studies have been reported in these aspects.

The main objective of this study is to extract amorphous and crystalline nano silica from MG by acid leaching and sol gel method. This study helps us not only to prepare valuable silica powder but also to alleviate the ecological problems caused by MG, thus making it a value-added product. Both crystalline and amorphous silica are important in the field of material science [26]. Temperature has a significant effect on the crystalline nature of silica [27]. Thus, studies were carried out at the most suitable temperature. The morphology and purity of silica also depend on the method adopted for preparation. Thus, comparatively easier method acid leaching and time-consuming method sol gel process were adopted, and the crystallinity, structural elucidation, morphology, purity, and thermal stability were studied by XRD, FT-IR Spectroscopy, FESEM-EDS and TG analysis.

2 Materials and Methods

2.1 Materials

The Mission Grass (MG) collected from roadsides of Kerala, India, Hydrochloric Acid (HCl), Sodium Hydroxide (NaOH), Silver nitrate ($AgNO_3$), Whatmann No 1 filter paper all procured from Sigma Aldrich. All the chemicals are of the best grade and were used without further purification.

3 Methods

3.1 Synthesis of Amorphous Silica

3.1.1 Washing and Drying

MG collected is cut into small pieces, washed with water to remove dust and mud. It is dried under sunlight for a day. The dried leaves are grounded well, and the powder is sieved through 40 mm mesh. 20 g of dried, powdered MG is heated in a muffle furnace at 600 °C for 20 h, yielded 1.4 g (7%) mission grass ash (MGA).

3.1.2 Formation of 600 °C Acid Leached Silica (600ALS)

1 g MGA is digested with 2 N HCl for 5 h using a magnetic stirrer kept at 200° C. It is then heated in a Bunsen burner for 45 min. HCl is added at regular intervals to compensate for the loss due to evaporation. This is then kept in a water bath overnight and filtered through Whatman No 1 filter paper. The residue is washed with hot water till the washings are free from chloride ion. The residue is dried in an air oven at 150 °C and the process yields 0.6-g (4.2% of MG) product. The dried residue is characterized by XRD, FT-IR and FESEM-EDS.

3.1.3 Synthesis of 600 °C Sol Gel Silica (600 SGS)

1 g of 600ALS is digested with 3 M NaOH, since percentage yield of pure silica is higher with 3 M NaOH [28] in a magnetic stirrer at 80° for 5 h. It is then kept overnight and filtered through Whatman No 1 Filter paper. To the filtrate, which is assumed to be sodium silicate (Na_2SiO_3), 2 M HCl is added drop wise with constant stirring, till a white gelatinous precipitate is formed [29]. It is allowed to settle for 12 h and then filtered. The precipitate is washed several times with hot water and then with cold water to ensure the removal of all soluble impurities. The gel thus obtained is heated in an air oven at 150 °C for 3 h. The yield of the as-synthesized sample is found to be 0.4 g (1.68% of MG).

3.2 Synthesis of Crystalline Silica

The same procedure is adopted for the synthesis of 850 °C Acid Leached Silica (850ALS) and 850 °C Sol Gel Silica

(850SGS). But the washed, dried, powdered MG is heated in a muffle furnace for 850 °C for 20 h. The yield of MGA is 1.1 g (5.5%), 850ALS is 0.59 g (3.25% of MG) and 850SGS is 0.23 g (1.25% of MG) respectively. Both are characterized and their comparative studies are done. All steps involved in the process is shown in Fig. 1.

4 Characterization Techniques

Silica samples were characterized by XRD, FT-IR, TG and FESEM-EDS analysis. X -Ray Diffraction studies were performed on a X'pert^3 Powder Diffractometer using Cu K_α radiation at a wavelength of 1.54 Å. Generator voltage is 45 k V and tube current is 30 m A. Scanning range is 2θ value 5° to 80° and step size is 0.017. Background correction has been done. FT-IR spectra were recorded using Agilent Technologies Carry 660 instrument with KBr pellets in the wave number region of 400–4000 cm^{-1}. Thermal stability of 600SGS and 850SGS were determined by Perkin- Elmer's STA 8000 instrument with a temperature range of 30 °C to 1100 °C at a heating rate of 10 °C/minute in an inert atmosphere of nitrogen. Morphological studies and chemical composition are determined by FESEM-EDS, and the instrument used was Carl Zeiss-Sigma by sputtering silica powder with gold.

5 Results and Discussion

5.1 Fourier Transform-Infra Red (FT-IR) Spectroscopy

The presence of silica in different samples are confirmed by FT-IR spectra, which was taken in transmittance mode. Figure 2a-d shows the FT-IR spectra of 600ALS, 850ALS, 600SGS and 850SGS respectively. All the samples have prominent and characteristic peaks at fingerprint region. Spectra matches with the silica that is obtained from tetra ethyl ortho silicate precursor [30]. The main chemical groups in silica are silanol and siloxane [31]. The absence of peak between 2800 cm^{-1} and 3000 cm^{-1} shows that all samples are free from organic components [32] Fig. 2a shows the FT-IR spectrum of 600ALS. The most intense peak at 1078 cm^{-1} is due to the asymmetric stretching of Si–O-Si bond and the less intense band at 795 cm^{-1} is due to symmetric stretching of Si–O-Si bond [33]. Medium intense peak at 470 cm^{-1} corresponds to the rocking vibration of Si–O-Si bond [34]. The peak at 1641 cm^{-1} is attributed to O–H bending motion of silanol group or adsorbed water molecule [35]. A broad peak around 3500 cm^{-1} is attributed to the hydrogen bonded O–H group of silanol or adsorbed H_2O molecule [36].

Figure 2b shows the FT-IR spectra of 850ALS which is similar to that of 600ALS, but Fig. 2b has a more pronounced IR band with narrow line width. This indicates the more crystalline nature which was further confirmed by XRD. The prominent peak at 1090 cm^{-1} is due to asymmetric stretching and other characteristic peaks at 792 cm^{-1} and 477 cm^{-1} are attributed to symmetric stretching and rocking vibration of Si–O-Si bond. The peak at 1627 cm^{-1} which is attributed to O–H bending motion diminishes and the peak at 3442 cm^{-1} becomes very narrow compared to that of 600ALS. This is because calcination at higher temperature leads to more dehydration of silanol and desorption of water molecules from the compound. The distinct peak which is found in both 850ALS and 850SGS is assumed to be due to the stretching vibration of Si–C bond. This is since silicon in the grass, which is bonded with organic parts, will be converted to carbides at high temperature calcination [37]. Figure 2c shows the FT-IR spectrum of sol gel silica which is extracted from 600 °C heated MGA followed by acid leaching. The spectrum is entirely different from the other three. The broad and rounded peaks are typical of those amorphous solids. Prominent peaks are at 1056 cm^{-1}, 803 cm^{-1} and 465 cm^{-1} which are characteristic peaks of silica [38]. The intensity of the peak at 1641 cm^{-1}, which is due to the O–H bending, is higher than that in other spectra and this confirms the hydrophilic surface of silanol group [39]. A small peak at 951 cm^{-1}, which is absent in other spectra, is attributed to Si–H bending [40]. There

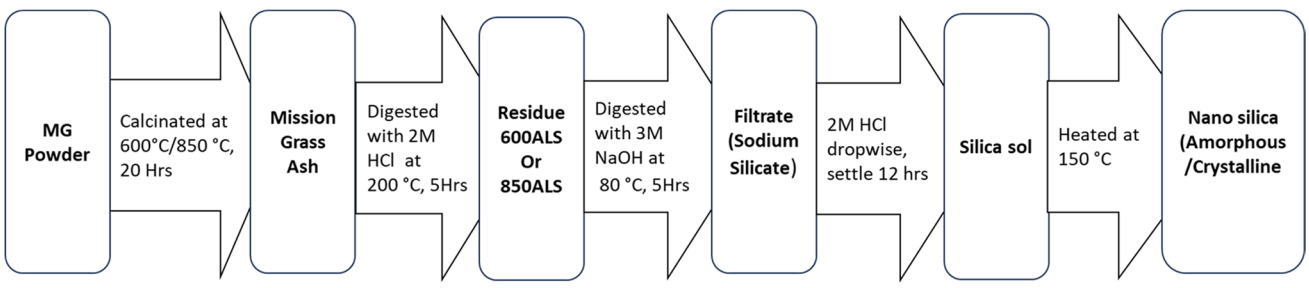

Fig.1 Schematic Representation of synthesis of Amorphous and Crystalline Nano silica from Mission Grass

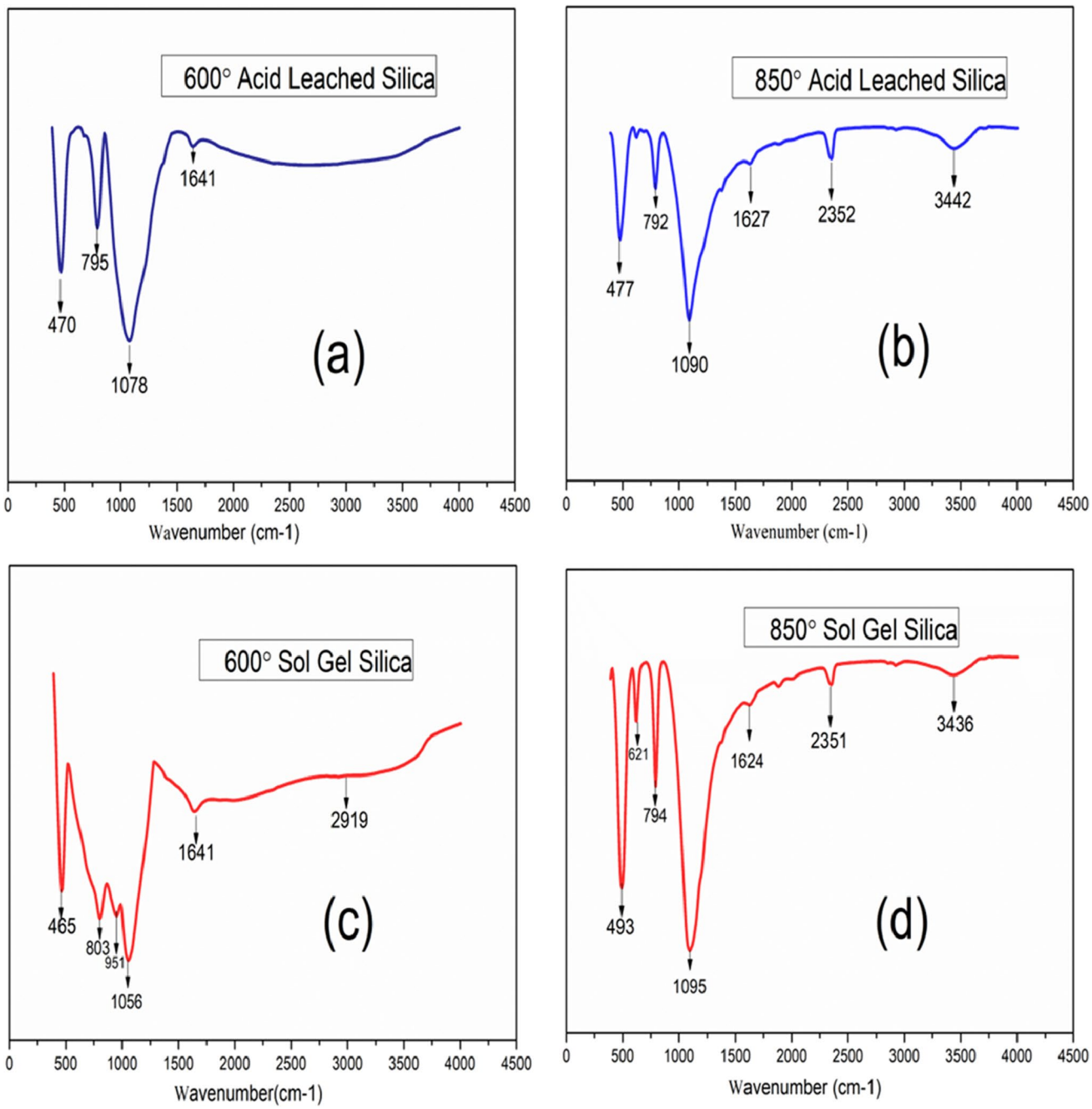

Fig. 2 FT-IR spectra of (**a**) 600ALS (**b**) 850 ALS (**c**) 600SGS (**d**) 850SGS

is no peak at 2350 cm^{-1} which rules out the existence of Si–C bond and indicates that the compound is pure. This was further confirmed by XRD. The broad band due to O–H stretching becomes much more diffused and irregular. This is because in 600SGS O–H group is extensively H-bonded due to silanol group and adsorbed water molecule [41].

Figure 2d shows the spectrum of 850SGS in which all the peaks are very sharp and narrow due to crystalline nature, which was further confirmed by XRD studies. The characteristic peaks of silica are present at 493 cm^{-1}, 794 cm^{-1}, and 1095 cm^{-1}. The peaks at 1624 cm^{-1} and 3436 cm^{-1}, which are due to the bending and stretching modes of O–H group, prevail even though the sample was calcinated at higher temperature. This is due to the presence of physically adsorbed water molecule from the environment [42]. This peak appears to be narrower due to dehydration of silanol groups and rupturing of H-bonds.

5.2 X-Ray Diffraction (XRD) Analysis

Figure 3a-f shows the X-ray diffractograms of different forms of silica at different temperature of calcination and through different methods of preparation

Figure 3a and b show the X-ray diffraction pattern of MGA obtained by heating the dried grass at 600 °C and 850 °C respectively. During calcination at high temperature, almost all organic content will be removed but this will lead to crystallization of some ash, both Fig. 3a and b show this behaviour. The crystalline parts of the ash exist in the form of cristobalite, tridymite and quartz. The peaks at 2θ = 21.9°,28.2°, 31.5° and 36.1° is attributed to cristobalite [43]. The signals at 2θ = 20.8°,26.6°,49.3° and 60° is due to the presence of quartz form of silica [44]. The peaks at 23.3°, 27.8°, 30° and 36.1° is due to tridymite [45]. In Fig. 3b a greater number of peaks are found in the range of 2θ = 20°-35° which shows more crystalline nature at higher temperature.

Figure 3c and d are diffractogram of 600ALS and 850ALS respectively. Both are distinct in their appearance. Figure 3c is very broad with a few sharp peaks which shows its amorphous nature. Figure 3d has sharp peak only, which is clear evidence of crystallinity at higher temperature [38]. The prominent broad peak at 2θ = 21.9° is the characteristic of amorphous silica, which is like the peak observed for the amorphous silica extracted from rice husk [46, 47]. Some sharp peaks at 2θ = 26.6°, 49.9° and 60° is evidence for the existence of trace quantity of crystalline form quartz [44]. Heating at 850° C followed by acid leaching converts the silica content in the MG into crystalline form [48]. The major peak at 2θ = 21.8° is the characteristic of crystalline form and the minor peaks at 26.7°, 31.3° and 36° is attributed to the presence of other forms like crystoballite and tridymite, which are already discussed in the XRD of MGA.

Figure 3e and f shows the XRD of amorphous and crystalline forms of silica obtained by sol gel method. Figure 3e clearly indicates the amorphous nature of 600SGS. There is a broad hump from 15° -30° with a centered peak at 21.9° which confirms the formation of silica which is purely in amorphous form [49]. There are no other peaks found in the diffractogram, which shows the purity of the product and the absence of other minerals in the sample, as already found in the FT-IR of 600SGS.

Figure 3f shows that 850SGS is purely in crystalline nature, indicating cristobalite structure and is comparable with the silica obtained from sodium silicate [42]. The major peaks at 2θ = 21.9° and minor peaks at 28.5°, 31.5° and 36.3 is the clear evidence for the cristobalite structure for 850SGS [43]. The diffractogram is almost like 850ALS, but here the major peaks are more intense. The shoulder at major peak was diminished and some other peaks vanished, which suggests that 850SGS is purer than 850ALS. The XRD studies show that it is possible to isolate both amorphous and crystalline silica from MG either by acid leaching or sol gel method with high purity. Since the sol gel method is costlier and time consuming, we can adopt any method depending upon the purity of the product we require. The crystallinity index of different products is calculated and is given in the Table 1.

As per Table 1, 600SGS is highly amorphous which exists in the agglomerated form which will be later confirmed from FESEM image and has a lot of application in the realm's material science. Thus, MG is considered as a good source of amorphous silica and crystalline silica as well.

5.3 Thermogravimetry Analysis

Detailed thermal analysis of 600SGS and 850SGS was carried out from room temperature to 1100 °C. Figure 4a and b depict the thermogravimetry and corresponding differential thermogravimetry curves of 600SGS and 850SGS respectively. Both the samples show the rapid initial weight loss. This is due to the removal of physisorbed water i.e., moisture [50]. In the temperature range 30 °C-90°C the weight loss is 16% for 600SGS and 24% for 850SGS. This shows that crystalline silica is more hygroscopic than amorphous silica, hence crystalline silica can be used as a moisture absorber. The removal of physically bonded water is possible if heated up to 120 °C and if the sample contains micropores it will be retained even at higher temperature.

The second stage weight loss starts at 90 °C and ends at 330 °C. At this stage, weight loss is 4.2% and 3.4% for 650SGS and 850SGS respectively. This weight loss is attributed to the removal of internal water and from silanol group [51]. Silica, on heating hydrogen bonded hydroxyl group will be removed quickly in the temperature range 200–400 °C and isolated hydroxyl group will be removed only at higher temperature [52]. The weight loss percentage shows that the amorphous silica has more internal water due to its more porous nature. A small dip at 370 °C in both samples is due to decomposition of any carbonaceous matter present in the sample. In the third stage both the curve has constant slope up to 700 °C, then slope begins to decrease and becomes parallel to X- axis shows that both the silica is thermally stable at higher temperature.

The number of hydroxyl groups present in the sample is also calculated. It is obtained by measuring the difference in weight percentage of the sample at which all physisorbed water molecule is removed and at the end point of the measurement [52].

It is given by Eq. (1)

$$nO - H\left(SiO_2\right) = \frac{2\left\{W\left(T_0\right) - W\left(T_{final}\right)\right\} \times 10}{MH_2O} \quad (1)$$

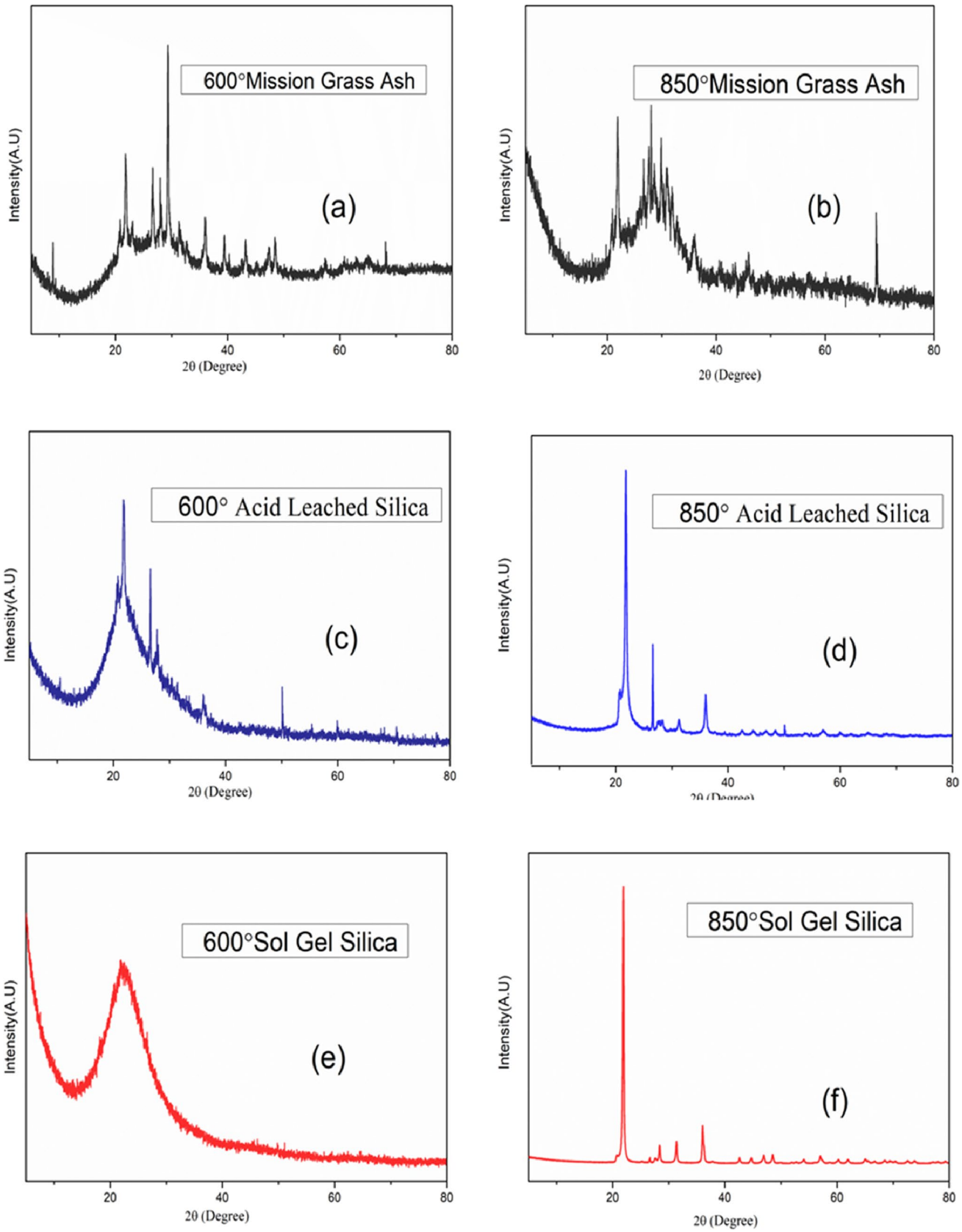

Fig. 3 X-Ray diffraction patterns of (**a**) 600MGA (**b**) 850MGA (**c**) 600ALS (**d**) 850ALS (**e**) 600SGS (**f**) 850SGS

Table 1 Crystallinity index of 600ALS, 600SGS, 850ALS and 850SGS

Sample	Crystallinity Index
600ALS	51.4%
600SGS	43%
850ALS	59%
850SGS	82%

where *n* O–H is the number of moles of O–H group, $W(T_0)$ and W (T_{final}) is the weight percentage at 90 °C and 1100 °C (current study) respectively and M H_2O is the molecular weight of water.

Here the number of O–H group calculated from the thermogram is 12.6 m mol/gram and 10 m mol/gram for amorphous silica and crystalline silica respectively.

Figure 4b shows the DTG curves of 600SGS and 850SGS, both are almost similar graphs. Initial weight loss is very high up to 100 °C due to the removal of moisture content, since silica is hygroscopic. There is no observable weight loss from 125 °C to 250 °C (300 °C for 850SGS) then there is a sharp dip in the curve which is attributed to decomposition of any of the organic matter and then both curve is almost parallel to X- axis [53]. This shows that a steady weight loss occurs in both cases due to removal water from silanol group [54]. The heat changes during thermogravimetric analysis of 600SGS and 850SGS from room temperature to 1100 °C is recorded as DTA curve Fig. 4c. The graph shows that in the case of 600SGS up to 260 °C the process is endothermic due to desorption of water molecules in the sample. Then the process is exothermic, which is due to the condensation of Si–OH groups with the evolution of water molecules. But in the case of 850SGS, the process is endothermic up to 800 °C, which shows that there is a limited number of Si–OH group in the sample and the weight lost is prominently due to the desorption of water molecules.

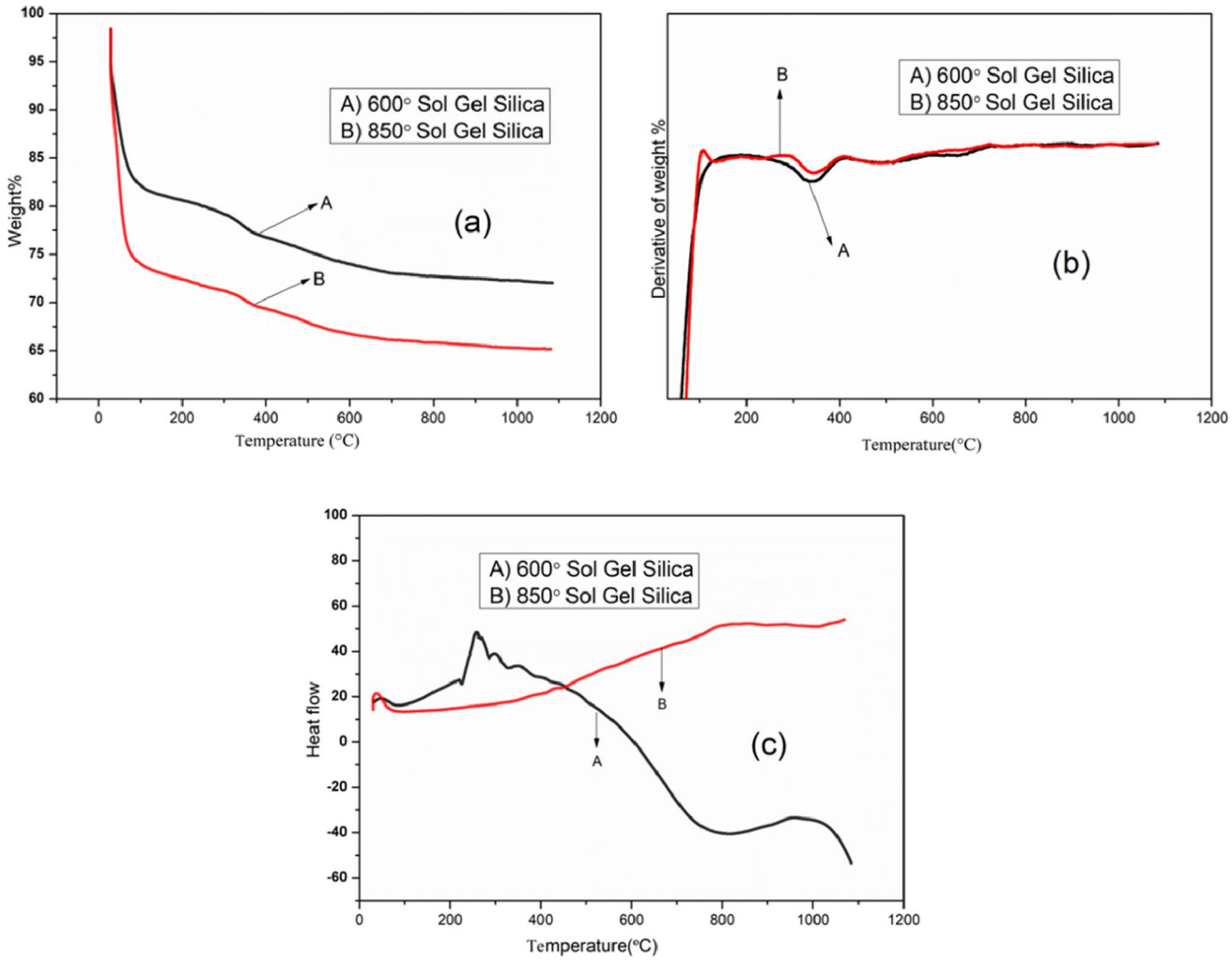

Fig. 4 (**a**) Thermogravimetry of 600SGS and 850SGS (**b**) DTG of 600SGSand 850SGS (**c**) DTA of 600SGS and 850SGS

5.4 Field Emission Scanning Electron Microscopy (FESEM) and Energy Dispersive X-ray Spectroscopy (EDS)

The morphology and chemical composition of the sample are studied using FESEM-EDS. Figure 5a-c shows the low as well as the high-resolution images and EDS data of 600ALS, 600SGS and 850 SGS respectively. The morphology of the silica obtained depends on the methodology and annealing temperature [55]. The irregular structures seen in all images are due to the formation of oxygenated siliceous compounds during annealing [56] FESEM images of 600 ALS (Fig. 5a) show that the silica nanoparticles are agglomerated and porous in nature with particle size in the range of 50 nm to 200 nm. Agglomeration of the particles are due to the strong intermolecular force between the silica particles. The porous nature of the silica particles is emerged due to the acid leaching and calcination of the organic matter during the synthesis. EDS data of 600 ALS shows a silica content of about 91.95% and the presence of minor percentages of impurities of the oxides of Na, K and Ca. It is interesting to notice the absence of Al oxide since the samples were subjected to vigorous acid leaching and repeated washing process. This process has offered the complete removal of Al as its water-soluble chlorides.

The FESEM images of 600SGS (Fig. 5b) show that particles have almost uniform size and the agglomeration is comparatively lesser than 600ALS and 850 SGS. The particle size is in the range of 20 -80 nm and a few associated microparticles are also found. EDS data shows that 600 SGS contains 95.61% of silica which is comparable to the studies reported for the extraction of silica from rice husk. 3.5% of Al_2O_3 is found in 600 SGS which is attributed to the conversion of Al ion into sodium aluminate. Sodium aluminate is soluble in water and will be precipitated as Al $(OH)_3$ during sol gel formation. The surface morphology of 850 SGS particles are found to be more compact in nature when compared with the other samples. Images shows that temperature have significant on the size of the particles [57].

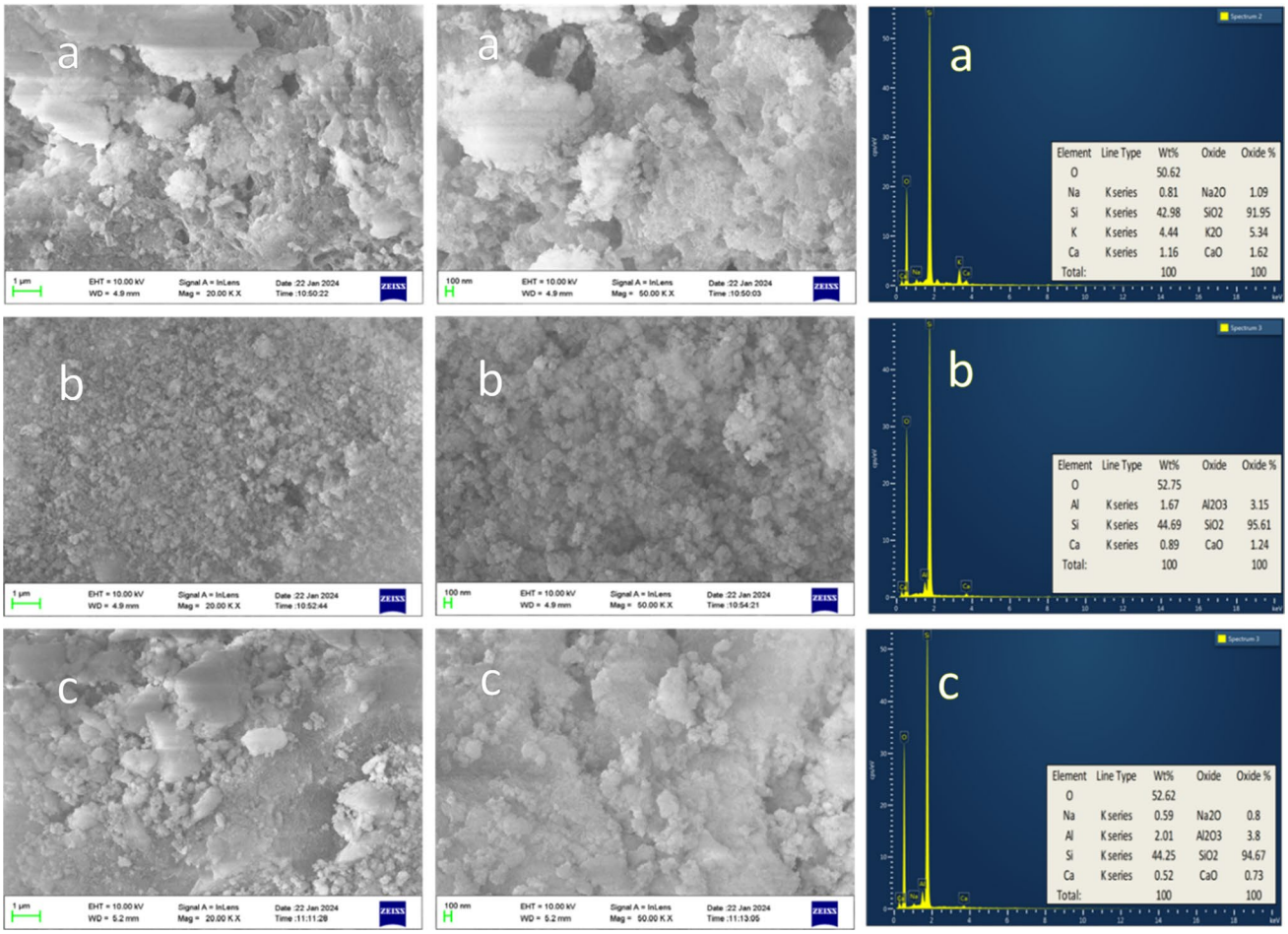

Fig. 5 FESEM and EDS of (**a**) 600ALS (**b**) 600SGS (**c**) 850SGS

6 Conclusion

A novel strategy for the synthesis of silica nanoparticles from MG is demonstrated. Acid leaching and sol gel method are utilized to obtain silica nanoparticles from MG. Amorphous and crystalline silica nanoparticles are obtained from MG by annealing the samples at 600 °C and 850 °C through both synthetic strategies respectively. The FT-IR studies show the presence of silica in all samples, the round, broad peaks of 600SGS shows its amorphous nature. XRD analysis shows that both 850ALS and 850SGS give sharp peaks, which indicates that calcination temperature has remarkable effect on the crystallinity of silica. Thermal studies show that crystalline silica is more hygroscopic than amorphous silica but later has more internal water due to its porous nature. DTA curve shows that the heating of 600SGS is endothermic at the beginning and then exothermic, but in the case of 850SGS, it is endothermic throughout heating which indicates a smaller number of Si–OH group. As per FESEM-EDS, nano sized, highly pure amorphous silica with less agglomeration can be synthesized by heating the MG at 600 °C followed by sol gel method. Thus, depending on the extent of purity required, nano silica can be synthesized from mission grass through a much cost effective acid leaching method than sol gel process. Finally, MG is not simply a fodder but a rich source of bio silica.

Author Contributions THAYYULLATHIL. and C.M. conducted the experiments and wrote the main manuscript. F.M. and E.K. analyzed the data. S.R. prepared the figures and tables. NADUPARAMBATH. supervised the whole studies. SASIDHARAN contributed in revision process. All authors reviewed the manuscript.

Funding This study has no financial fundings.

Data Availability The data presented in this study are available on request from the corresponding author.

Declarations

Ethics Approval and Consent to Participate Authors declare that the manuscript is not submitted to any other journal at the time of submission for consideration. Animals and Humans are not involved in the study.

Consent for Publication All authors agree to publish this article in the journal 'Silicon'.

Competing Interests The authors declare no competing interests.

References

1. Rossi LM, Shi L, Quina FH, Rosenzweig Z (2005) Stöber synthesis of monodispersed luminescent silica nanoparticles for bioanalytical assays. Langmuir 21:4277–4280. https://doi.org/10.1021/la0504098
2. Agrwal A, Kumar V, Kasana V (2021) Preparation and application of highly efficient and reusable TBAPIL@Si(CH2)3@nano-silica-based nano-catalyst for preparation of benzoxanthene derivatives. J Iran Chem Soc 18:2583–2595. https://doi.org/10.1007/s13738-021-02211-1
3. Rangaraj S, Venkatachalam R (2017) A lucrative chemical processing of bamboo leaf biomass to synthesize biocompatible amorphous silica nanoparticles of biomedical importance. Appl Nanosci (Switzerland) 7:145–153. https://doi.org/10.1007/s13204-017-0557-z
4. Bakhsheshi-Rad HR, Hamzah E, Kasiri-Asgarani M et al (2016) Structure, corrosion behavior, and antibacterial properties of nano-silica/graphene oxide coating on biodegradable magnesium alloy for biomedical applications. Vacuum 131:106–110. https://doi.org/10.1016/j.vacuum.2016.05.021
5. Vijayan M, Selladurai V, Balaganesan G, Suganya Priyadharshini G (2022) Comprehensive characterization of AA 2024T3 fiber metal laminate with nanosilica-reinforced epoxy based polymeric composite panel for lightweight applications. Polym Compos 43:8274–8296. https://doi.org/10.1002/pc.26998
6. Etli S, Yılmaz T, Hansu O (2024) Effect of White-Portland cement containing micro and nano silica on the mechanical and freeze-thaw properties of self compacting mortars. EngSci Technol Int J 50. https://doi.org/10.1016/j.jestch.2023.101614
7. Sun X, Xie J, Zhang J et al (2022) Hydrophobic Al2O3/SiO2/PDMS Composite Coatings for Anti-corrosion Application of 304 Stainless-Steel. J Inorg Organomet Polym Mater 32:4237–4249. https://doi.org/10.1007/s10904-022-02423-9
8. Green LJ, Bhatia ND, Toledano O et al (2023) Silica-based microencapsulation used in topical dermatologic applications. Arch Dermatol Res 315:2787–2793
9. Gao Y, Zhang Y, Hong Y et al (2022) Multifunctional Role of Silica in Pharmaceutical Formulations. AAPS PharmSciTech 23. https://doi.org/10.1208/s12249-022-02237-5
10. Sarkar P, Moyez SA, Dey A et al (2017) Experimental investigation of photocatalytic and photovoltaic activity of titania/rice husk crystalline nano-silica hybrid composite. Sol Energy Mater Sol Cells 172:93–98. https://doi.org/10.1016/j.solmat.2017.07.021
11. Hossain SKS, Mathur L, Roy PK (2018) Rice husk/rice husk ash as an alternative source of silica in ceramics: A review. J Asian Ceram Soc 6:299–313
12. Lv R, Peng J, Chen S et al (2017) A highly linear humidity sensor based on quartz crystal microbalance coated with urea formaldehyde resin/nano silica composite films. Sens Actuators B Chem 250:721–725. https://doi.org/10.1016/j.snb.2017.03.074
13. Balagna C, Perero S, Percivalle E et al (2020) Virucidal effect against coronavirus SARS-CoV-2 of a silver nanocluster/silica composite sputtered coating. Open Ceramics 1. https://doi.org/10.1016/j.oceram.2020.100006
14. Chruściel J, Ślusarski L (2003) Synthesis of nanosilica by the sol-gel method and its activity toward polymers. Mater Sci Pol 21(4):461–469
15. Deshmukh P, Bhatt J, Peshwe D, Pathak S (2012) Determination of silica activity index and XRD, SEM and EDS studies of amorphous SiO 2 extracted from rice Husk Ash. Trans Indian Inst Met 65:63–70. https://doi.org/10.1007/s12666-011-0071-z
16. Prabha S, Durgalakshmi D, Rajendran S, Lichtfouse E (2021) Plant-derived silica nanoparticles and composites for biosensors, bioimaging, drug delivery and supercapacitors: a review. Environ Chem Lett 19:1667–1691
17. Hassan AF, Abdelghny AM, Elhadidy H, Youssef AM (2014) Synthesis and characterization of high surface area nanosilica from rice husk ash by surfactant-free sol-gel method. J Solgel Sci Technol 69:465–472. https://doi.org/10.1007/s10971-013-3245-9

18. Lu P, Lo HY (2012) Highly pure amorphous silica nano-disks from rice straw. Powder Technol 225:149–155. https://doi.org/10.1016/j.powtec.2012.04.002
19. Firdaus MYN, Osman H, Metselaar HSC, Rozyanty AR (2016) Silica from lemon grass. .BioResources 11(1)1270–1279. https://doi.org/10.15376/biores.11.1.1270-1279
20. Shim J, Velmurugan P, Oh B-T (2015) Extraction and physical characterization of amorphous silica made from corn cob ash. J Ind Eng Chem 30:249–253. https://doi.org/10.1016/j.jiec.2015.05.029
21. Saed B, Ziaee M, Kiasat AR, JafariNasab M (2022) Preparation of nanosilica from sugarcane bagasse ash for enhanced insecticidal activity of diatomaceous earth against two stored-products insect pests. Toxin Rev 41:516–522. https://doi.org/10.1080/15569543.2021.1903038
22. Yusaidi NJ, Abdullah SA, Zarib NA (2020) X-ray diffractometer (XRD) and scanning electron microscopy (SEM) of silica extracted from banana stems via acid leaching treatment. In: IOP Conference Series: Materials Science and Engineering. Institute of Physics Publishing
23. Akpotu SO, Moodley B (2018) Effect of synthesis conditions on the morphology of mesoporous silica from elephant grass and its application in the adsorption of cationic and anionic dyes. J Environ Chem Eng 6:5341–5350. https://doi.org/10.1016/j.jece.2018.08.027
24. Miller I, Darwin B (2006) Management of mission grass(PennisetumPolystachion). Agnote, department of primary industry,fisheries and mines Northern Territory Government F38 1–9. http://www.nt.gov.au
25. Prasertwasu S, Khumsupan D, Komolwanich T et al (2014) Efficient process for ethanol production from Thai Mission grass (Pennisetum polystachion). Bioresour Technol 163:152–159. https://doi.org/10.1016/j.biortech.2014.04.043
26. Barik TK, Sahu B, Swain V (2008) Nanosilica - From medicine to pest control. Parasitol Res 103:253–258
27. Ülker S, Güden M (2022) The effect of the temperature of heat treatment process and the concentration and duration of acid leaching on the size and crystallinity of nano-silica powders formed by the dissociation of natural diatom frustule. Mater Express 12:1094–1107. https://doi.org/10.1166/mex.2022.2251
28. Thuadaij N, Nuntiya A (2008) Synthesis and characterization of nanosilica from Rice husk ash prepared by precipitation Method. J Nat Sci Special Issue on Nanotechnology 7.1(2008): 59–65
29. Vijayaraj S, Vijayarajan K (2023) Mechanical wear and hydrophobicity behaviour of Digitaria ischaemum fibre-reinforced finger millet husk biosilica toughened epoxy composites. Biomass Convers Biorefin. https://doi.org/10.1007/s13399-023-04638-3
30. Haque FZ, Nandanwar R, Singh P et al (2018) Effect of Different Acids and Solvents on Optical Properties of SiO2 Nanoparticles Prepared by the Sol-Gel Process. SILICON 10:413–419. https://doi.org/10.1007/s12633-016-9464-2
31. Rafiee E, Shahebrahimi S, Feyzi M, Shaterzadeh M (2012) Optimization of synthesis and characterization of nanosilica produced from rice husk (a common waste material). Int Nano Lett 2. https://doi.org/10.1186/2228-5326-2-29
32. Shadiya MA, Dominic CDM, Nandakumar N et al Isolation and Characterization of Fibrillar Nanosilica of Floral Origin: Cortaderia selloana Flowers as the Silica Source. https://doi.org/10.1007/s12633-021-01185-2/Published
33. Athinarayanan J, Periasamy VS, Alhazmi M et al (2015) Synthesis of biogenic silica nanoparticles from rice husks for biomedical applications. Ceram Int 41:275–281. https://doi.org/10.1016/j.ceramint.2014.08.069
34. Yadav VK, Fulekar MH (2019) Green synthesis and characterization of amorphous silica nanoparticles from fly ash. Mater Today Proc 18:4351–4359. https://doi.org/10.1016/j.matpr.2019.07.395
35. Guo Y, Wang YQ, Wang ZM, Shen CJ (2016) Study on the preparation and characterization of high-dispersibility nanosilica. Sci Eng Compos Mater 23:401–406. https://doi.org/10.1515/secm-2014-0010
36. Rafiee E, Shahebrahimi S (2012) Nano silica with high surface area from rice husk as a support for 12-tungstophosphoric acid: An efficient nano catalyst in some organic reactions. Chin J Catal 33:1326–1333. https://doi.org/10.1016/S1872-2067(11)60420-8
37. Krishnarao R V, Godkhindi MM (1992) Distribution of silica in rice husks and its effect on the formation of silicon carbide. Ceram Int 18(4):243–249. https://doi.org/10.1016/0272-8842(92)90102-J
38. Banoth S, Suresh Babu V, Raghavendra G et al Sustainable Thermochemical Extraction of Amorphous Silica from Biowaste. https://doi.org/10.1007/s12633-021-01293-z/Published
39. Sutha S, Sakthipandi K, Rajendran V et al (2012) Structural studies of nano silica employing on-line ultrasonic studies. Phase Transitions 85:565–576. https://doi.org/10.1080/01411594.2011.648933
40. Battisha IK, El Beyally A, El Mongy SA, Nahrawi AM (2007) Development of the FTIR properties of nano-structure silica gel doped with different rare earth elements, prepared by sol-gel route. J Solgel Sci Technol 41:129–137. https://doi.org/10.1007/s10971-006-0520-z
41. Gh Peerzada J Chidambaram R A Statistical Approach for Biogenic Synthesis of Nano-Silica from Different Agro-Wastes. https://doi.org/10.1007/s12633-020-00629-5/Published
42. Joni IM, Nulhakim L, Vanitha M, Panatarani C (2018) Characteristics of crystalline silica (SiO2) particles prepared by simple solution method using sodium silicate (Na2SiO3) precursor. Journal of Physics: Conference Series. Institute of Physics Publishing
43. Kordatos K, Gavela S, Ntziouni A et al (2008) Synthesis of highly siliceous ZSM-5 zeolite using silica from rice husk ash. Microporous Mesoporous Mater 115:189–196. https://doi.org/10.1016/j.micromeso.2007.12.032
44. Chisholm J (2005) Comparison of quartz standards for X-ray diffraction analysis: HSE A9950 (Sikron F600) and NIST SRM 1878. Ann Occup Hyg 49:351–358. https://doi.org/10.1093/annhyg/meh095
45. Prasetyoko D, Ramli Z, Endud S et al (2006) Conversion of rice husk ash to zeolite beta. Waste Manage 26:1173–1179. https://doi.org/10.1016/j.wasman.2005.09.009
46. Ma X, Zhou B, Gao W et al (2012) A recyclable method for production of pure silica from rice hull ash. Powder Technol 217:497–501. https://doi.org/10.1016/j.powtec.2011.11.009
47. Ali HH, Hussein KA, Mihsen HH (2023) Antimicrobial Applications of Nanosilica Derived from Rice Grain Husks. SILICON 15:5735–5745. https://doi.org/10.1007/s12633-023-02467-7
48. Bheel N, Fareed &, Memon A, Meghwar SL Study of Fresh and Hardened Properties of Concrete Using Cement with Modified Blend of Millet Husk Ash as Secondary Cementitious Material. https://doi.org/10.1007/s12633-020-00794-7/Published
49. Ali HH, Mihsen HH, Hussain KA (2023) Synthesis, Characterization and Antimicrobial Studies of Modified Silica Materials Derived from Rice Husks. Bionanoscience 13:1163–1176. https://doi.org/10.1007/s12668-023-01144-8
50. Sarangi M, Bhattacharyya S, Behera RC (2009) Effect of temperature on morphology and phase transformations of nano-crystalline silica obtained from rice husk. Phase Transitions 82:377–386. https://doi.org/10.1080/01411590902978502

51. Huang M, Cao J, Meng X et al (2016) Preparation of SiO2 nanowires from rice husks by hydrothermal method and the RNA purification performance. Chem Phys Lett 662:42–46. https://doi.org/10.1016/j.cplett.2016.09.012
52. Ek S, Root A, Peussa M, Niinistö L (2001) Determination of the hydroxyl group content in silica by thermogravimetry and a comparison with 1H MAS NMR results. Thermochim Acta 379:201–212. https://doi.org/10.1016/S0040-6031(01)00618-9
53. Yu LY, Huang ZX, Shi MX (2014) Synthesis and characterization of silica by sol-gel method. In: Advanced Materials Research. Trans Tech Publications Ltd, pp 189–192
54. Kurbanov M, Tulaganov S, Nuraliev U et al (2023) Comparative Characteristics of the Structure and Physicochemical Properties of Silica Synthesized by Pyrogenic and Fluoride Methods. SILICON 15:1221–1233. https://doi.org/10.1007/s12633-022-02087-7
55. Karumanchi M, Nerella R, Mikkili I (2022) An integrated approach on extraction methodologies of nanosilica from cultivated agricultural wastes and microstructural characteristics – A review. Mater Today Proc 62:2883–2891. https://doi.org/10.1016/j.matpr.2022.02.476
56. Rodríguez-Díaz JM, García JOP, Sánchez LRB et al (2015) Comprehensive Characterization of Sugarcane Bagasse Ash for Its Use as an Adsorbent. Bioenergy Res 8:1885–1895. https://doi.org/10.1007/s12155-015-9646-6
57. Morales-Paredes CA, Rodríguez-Linzán I, Saquete MD et al (2023) Silica-derived materials from agro-industrial waste biomass: Characterization and comparative studies. Environ Res 231. https://doi.org/10.1016/j.envres.2023.116002

Authors and Affiliations

Ajmal Thayyullathil[1] · C. M Naseera[1] · F. M Liyakhath[1] · E. K Vydhehi[1] · S. R Sheeja[1] · Subair Naduparambath[1] · Swetha Sasidharan[2]

✉ Ajmal Thayyullathil
ajmalthayyullathil@gmail.com

[1] Department of Chemistry, Govt. College Madappally, Vadakara, Kozhikode, Kerala, India

[2] Department of Chemistry, R. Sankar Memorial SNDP Yogam Arts and Science College, Koyilandy, Kerala, India